Quantum Electronics **47** (10) 901–905 (2017)

https://doi.org/10.1070/QEL16437

Variation in the structure of a time-dependent SRS spectrum in microfiltered water

V.A. Babenko, N.F. Bunkin, A.A. Sychev

Abstract. **The time-dependent stimulated Raman scattering of light in water subjected to structural transformation by track membrane microfiltration is investigated. It is shown that the probability of SRS at the frequency of the ice spectral component in the band of stretching OH vibrations of water molecules decreases as a result of water filtration.**

Keywords: *water structure, molecular complexes, nonlinear light scattering.*

1. Introduction

Water is a complex configuration of different structural elements, which arise as a result of intermolecular interactions and, in particular, hydrogen bonding. According to the modern concepts, water in liquid state is a mixture of ice-like structures (hexagonal ice Ih), diamond-like tetramers and small-size complexes (dimers, trimers, etc.), and water monomers. The existence of hexagonal ice structure Ih in liquid water was revealed in [1] during spectroscopic analysis of small-angle scattering of X-ray synchrotron beams in the water volume; this feature was described in detail in [2]. A similar conclusion was drawn in [3] as a result of spectroscopic study of spontaneous Raman scattering in water. It was established that molecular complexes with vibrational frequencies of ~3600 and 3450 cm^{-1}, as well as with a frequency of ~3200 cm^{-1} (characteristic of ice-like hexamers), exist in water up to the boiling temperature. The existence of a typical ice structure near water surface (with a characteristic frequency of ~3200 cm^{-1}) was found in [4], where the generation of the sum frequency in the radiation reflected from a water surface exposed to two laser pulses with different frequencies was analysed. A similar result was obtained when generating the second harmonic in case of reflection from water surface in [5], where the absence of central symmetry of water in the surface layer, caused by the alignment of molecules at the air–water interface, was indicated. Note also that the existence of at least two characteristic structural fractions in water was also established by Walrafen [6] based on the presence of the isosbestic point in the spontaneous Raman spectrum recorded with variation in temperature. The Raman spectrum in the frequency range from 3200 to 3600 cm^{-1} corresponds to stretching OH vibrations of water molecules. The spectrum is a wide band with a weakly pronounced structure, determined by the molecules entering different structural water complexes. A computer analysis of this band made it possible to reveal components with frequencies of ~3247, 3435, 3535, and 3622 cm^{-1}. Furthermore, Colles et al. [7] proposed for the first time to use SRS in water for more detailed structural analysis of molecular complexes.

However, the experiments on observation of SRS in water [7–10] upon excitation by a train of ultrashort laser pulses showed that SRS characteristics are described from the point of view of macroscopic theory, which presents parameters of a medium as the result of averaging of contributions of different molecular complexes entering the ensemble. At the same time, the characteristic times of their structural transformations are known to lie in the picosecond range. For example, the lifetime of the hydrogen bond, estimated from the degree of depolarisation of Rayleigh scattering [11], is ~0.5 ps at room temperature and the orientational transformation time of molecules is ~1 ps [12]. The variety of molecular structures in water is determined to a great extent by the presence of the hydrogen bond between individual molecules and by the interaction of molecules in the boundary layers of the air–water interface. Taking into account the short transformation time of molecular complexes, it appears possible to reveal specific features of the microscopic structure of water by the SRS method in the field of specifically single ultrashort laser pulse.

Recently, the researchers studying the water structure have paid much attention to gaseous nanoobjects: bubbles stabilised by ions (bubstons) [13, 14]. A bubston is a relatively stable gas bubble 10–100 nm in size, whose mechanical stability is due to the balance of compressive surface tension forces and tensile Coulomb forces, which are induced by ions of certain type specifically adsorbed into the bubston shell. As was shown in [15], these are most often electrolyte anions. Since they have the same sign, a ponderomotive force arises to stretch the bubble. The external bubston shell is formed by cations present in the solution. On the whole, a bubston with a double electric layer in the ion shell is an electrically neutral complex, as was confirmed in [15] by theoretical calculations of the charge density in the vicinity of a bubston using the Poisson–Boltzmann theory. In addition, a direct proof of the bubston existence in aqueous solutions was their detection by phase microscopy [16]. As a result of a peculiar interaction (intercoagulation), these nanoscale bubstons can form the so-called bubston clusters with a characteristic size of ~1 μm.

V.A. Babenko P.N. Lebedev Physical Institute, Russian Academy of Sciences, Leninsky prosp. 53, 119991 Moscow, Russia;
N.F. Bunkin N.E. Bauman Moscow State Technical University, Vtoraya Baumanskaya ul. 5, 105005 Moscow, Russia;
A.A. Sychev P.N. Lebedev Physical Institute, Russian Academy of Sciences, Leninsky prosp. 53, 119991 Moscow, Russia; N.E. Bauman Moscow State Technical University, Vtoraya Baumanskaya ul. 5, 105005 Moscow, Russia; e-mail: sychev4@yandex.ru

Received 24 May 2017; revision received 6 July 2017
Kvantovaya Elektronika **47** (10) 901–905 (2017)
Translated by Yu.P. Sin'kov

Bubstons in chemically pure water are stabilised by negatively charged OH^- anions adsorbed on their inner surface [17]. The adsorption of OH^- ions may lead to the alignment of water ions on the bubston surface into some ordered structure, which is apparently similar to the structure formed on the air–water interface.

The purpose of this study was to describe the microscopic structure of water. To this end, we investigated (taking into account the dynamic character of water molecular structures and their short transformation time) the specific features of SRS in water in the field of a single ultrashort (picoseconds) laser pulse.

2. Experimental

The initial radiation was in the form of a single 15-ps pulse of the second optical harmonic (λ = 532 nm), obtained by conversion of a pulse selected from a pulse train generated by a passively Q-switched Nd^{3+}:YAG laser (λ = 1064 nm).

To observe nonlinear scattering in water, we developed a laser setup based on a passively Q-switched YAG:Nd^{3+} active element, which generated picosecond laser pulses. A schematic of the experimental setup is presented in Fig. 1. The master oscillator cavity was formed by end mirrors M1 and M2, rotational mirror M3, and polarisation prism P. Highly reflecting mirror M1 (with reflectance R = 100%) had a radius of curvature of 2.5 m. The use of this mirror made it possible to obtain stable generation of the TEM_{00q} mode. End mirror M2 was a passively Q-switched cell (filled with dye No. 3262 in ortho-dichlorobenzene) based on a plane mirror (R = 100%). Stable generation of ultra-short laser pulses with a duration of ~20 ps was implemented using the regime in which the active-medium gain saturation coincided in time with the passive gate bleaching (the so-called second generation threshold regime) [18].

The initial vertical polarisation of laser radiation was provided by DKDP-based polarisation prism P. Electro-optical modulator M was used to select a single USLP from a pulse train. When a high-voltage electric pulse with a duration equal to the laser-beam axial period was applied to the modulator, the plane of polarisation of the laser radiation rotated by 90°. This radiation was extracted from the cavity by polarisation prism P. Rotational mirrors M4 and M6 were applied to direct the single pulse to amplification cascade AC. After amplification, the maximum energy of a single USLP with λ = 1064 nm, average duration of ~20 ps, and spectral width of ~0.8 cm^{-1} was 3 mJ. The output beam diameter was 1 mm. Then this radiation was converted (using a KDP crystal) into the second harmonic (λ = 532 nm), filtered by filter F1, and focused by lens L1 with a focal length F_1 = 100 mm to a cell C filled with water (the cell length was 20 mm). The shape of the second-harmonic pulse was recorded using photoelectron recorder PER with a time resolution of 6 ps. Figure 2 shows a typical PER image of a 15-ps USLP (λ = 532 nm) formed in the above-described system.

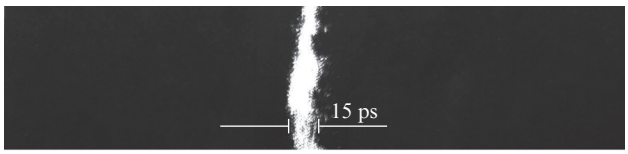

Figure 2. PER image of a second-harmonic USLP (λ = 532 nm).

The visible light emerging from water-filled cell C in the laser-beam propagation direction was focused by lens L2 on the input slit of miniature spectrometer SP with a spectral resolution of $\delta\nu$ = 20 cm^{-1}. Along with the analysis of the nonlinear scattering spectra along the laser beam direction, we recorded (using photodetector PD) the scattered radiation from a track at an angle of 90° to the incident beam.

The experiments were performed with deionised water having a resistivity of 5 MΩ cm, purified from solid microparticles and external ionogenic impurities. At the same time, as was noted above, this water may be inhomogeneous due to the presence of bubston clusters (stable particles consisting of bubstons), which may lead to additional structurisation of water molecules on the air–water interface with the formation of an ice-like structure. In turn, bubston clusters, as well as bubstons, may cause additional light scattering with an intensity greatly exceeding that of Rayleigh scattering from water molecules. At the same time, it was found that the number of bubstons and bubston clusters can be reduced using the technique of track membrane microcapillary filtering, which was applied by us. A 15-μm-thick membrane plate had many tracks with a hole diameter of ~0.4 μm. Figure 3 shows the dependence of the light intensity scattered in the water subjected to this filtering on the filtering time. The initial intensity level corresponds to water contacting with atmosphere for a long time (no less than 24 h). It can be seen that this microcapillary filtering in the regime of drop-by-drop penetration of water through the cell in the absence of contact with atmosphere led to a decrease in the light intensity scattered in water by a factor of more than 10. The water became more optically homogeneous, with a low bubston concentration and the absence of visible scattering centres (micrometer-sized air bubbles). Thus, the track membrane microfiltration allowed us to study both the water contacting with atmosphere for a long time and containing bubstons and bubston clusters and the

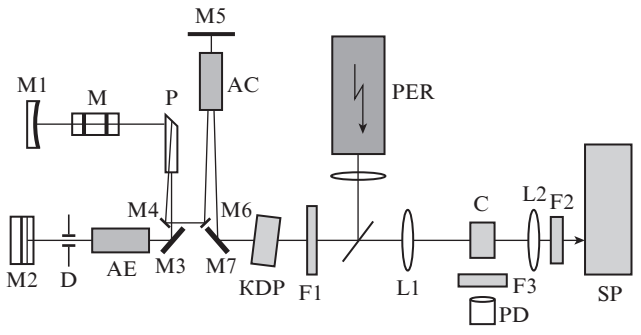

Figure 1. Schematic of the setup for recording nonlinear light scattering in water:
(AE) YAG:Nd^{3+} active element (4 mm in diameter and 73 mm long); (M1) highly reflecting mirror (R = 100%); (M2) passively Q-switched cell based on mirror (R = 100%); (P) polarisation prism; (M) electro-optical modulator (DKDP crystal); (D) 2.5-mm diaphragm; (M3–M7) folding mirrors (R = 100%); (AC) amplification cascade (YAG:Nd^{3+} crystal, 6 mm in diameter and 80 mm long); (PER) photoelectron recorder; (L1) lens with F_1 = 100 mm; (L2) lens with F_2 = 30 mm; (F1) filter cutting off laser radiation with λ = 1064 nm; (F2) filter cutting off second-harmonic excitation radiation with λ = 532 nm; (F3) filter transmitting only radiation with λ = 1064 nm; (PD) photodetector; (SP) spectrometer; (C) cell.

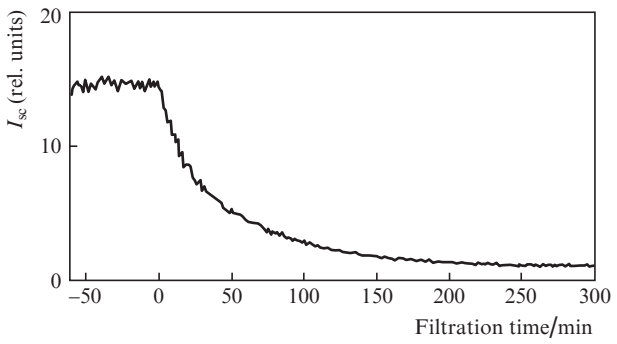

Figure 3. Dependence of the intensity of light scattered in water subjected to track membrane microcapillary filtration on the filtration time ($T \geqslant 0$). The initial intensity level ($T \leqslant 0$) corresponds to water contacting with atmosphere for a long time.

water purified to a great extent from these components as a result of microfiltration.

The experiments with observation of SRS both in filtered water and in water contacting with atmosphere showed that the SRS arises on molecular OH stretching vibrations in the frequency range of 3200–3500 cm^{-1}. Here, independent of the excess of pumping level over the threshold value, SRS occurs only in the forward direction. The fact that this regime of SRS in water is implemented under our conditions of SRS excitation by a single picosecond pulse with a duration $\Delta t \approx 15$ ps indicates that the SRS formation has a non-stationary character when $v\Delta t \leqslant l$ (l is the waist length in the lens caustic and v is the speed of light in water). Figure 4 shows an SRS pattern in the far-field zone, recorded in the lens focus. It can be seen that the divergence of scattered radiation does not exceed 35 mrad.

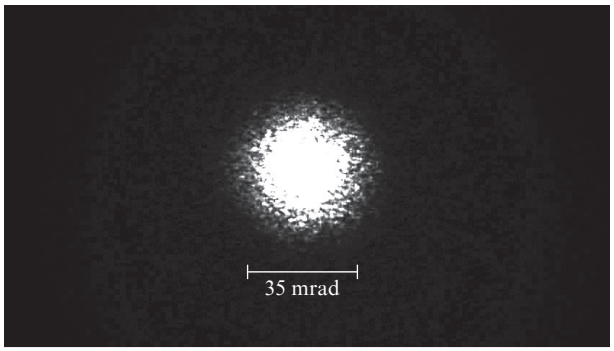

Figure 4. SRS pattern in water, recorded in the far-field zone near the SRS threshold (irradiation by a 15-ps pulse).

The first experiments on studying the SRS spectra at the SRS threshold were performed on water contacting with atmosphere. Figure 5 shows the characteristic SRS spectra for this water. Each spectrum was recorded upon SRS excitation by a single USLP. It can be seen that the SRS spectrum in each case is a set of single lines, whose frequencies change from pulse to pulse, while the frequency range of the SRS radiation is within the spectral profile of spontaneous Raman scattering on OH stretching vibrations of water molecules (ν = 3000–3700 cm^{-1}).

The Raman scattering spectrum in the range of OH stretching vibrations of water molecules is generally a set of time- and ensemble-averaged scattering profiles of individual structural molecular complexes of hexagonal ice (Ih) type, tetramers and small-size objects (dimers, trimers, etc.), and water monomers. This inhomogeneous broadening of the Raman line reflects the distribution of the vibrational frequencies of molecular complexes and the inhomogeneity of their local environment. At the same time, the dynamics of structural changes, occurring mainly during the transformation of hydrogen bonds between water molecules, leads to a change in the instantaneous distribution of vibrational frequencies, which is characteristic of dynamic inhomogeneous broadening. Since these fluctuations occur in the picosecond range, they can be detected when observing the SRS spectra excited by single picosecond pulses. In our case, the SRS in water is formed for a time Δt = 15 ps (λ = 532 nm). As follows from Fig. 5, the SRS spectra of water contacting with atmosphere, excited by single picosecond pulses, arise at different frequencies.

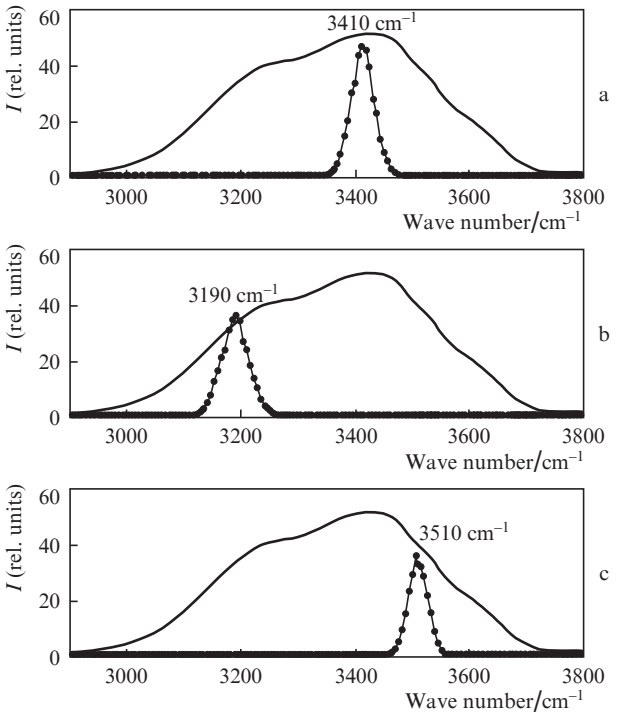

Figure 5. SRS spectra, recorded upon excitation by single picosecond pulses in water contacting with atmosphere: (circles) signals from detecting elements of multichannel recording matrix with a spectral step of ~6 cm^{-1} per channel (measurement error is less than 10% of measured signal) and (solid lines) profiles of spontaneous Raman scattering in the range of OH stretching vibrations (according to the data of [6]).

Figure 6a shows a histogram of SRS line frequencies for water contacting with atmosphere. This histogram characterises the SRS probability at different frequencies for a series of laser shots. The interval of frequency sampling and statistical averaging was chosen to be 20 cm^{-1}. As follows from Fig. 6a, the SRS probability is maximum for the SRS at a frequency $\nu \approx 3400$ cm^{-1} in the vicinity of the maximum of the spontaneous Raman scattering spectrum. At the same time, a noteworthy feature is the existence of SRS in the frequency range near

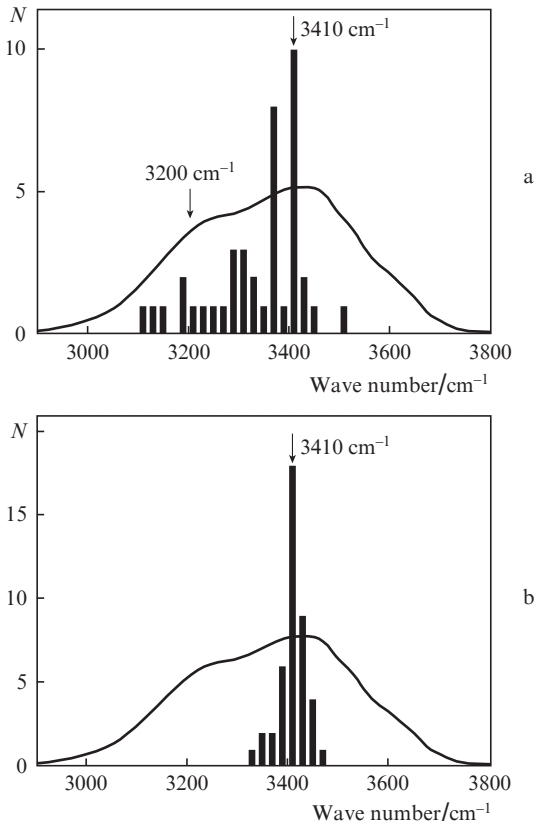

Figure 6. Histograms of the number of realisations N of line frequencies in the SRS spectra of (a) water contacting with atmosphere and (b) water subjected to track membrane microfiltration. Each spectrum is obtained upon SRS excitation by a single picosecond pulse with λ = 532 nm. Solid lines are profiles of spontaneous Raman scattering in the range of OH stretching vibrations (according to the data of [6]).

$\nu \approx 3200$ cm^{-1}, which is characteristic of ice-like hexamers. In accordance with our hypothesis, the formation of these structures is related to the presence of bubstons and bubston clusters in water. The concentration of these objects could be significantly reduced by applying microcapillary filtration (Fig. 3). This technique implies slow transmission of water through a large number of microcapillaries. The thus processed water gradually flew through cell C, and further SRS analysis was performed on this filtered (capillary) water.

The corresponding histogram of SRS line frequencies for filtered water is presented in Fig. 6b. As in the case of the water contacting with atmosphere, the SRS spectrum of the water subjected to microcapillary filtering is a single line at the SRS threshold. The maximum SRS probability, as previously, lies in the frequency range near $\nu \approx 3400$ cm^{-1}. However, SRS was not observed at frequencies $\nu \approx 3200$ cm^{-1}. This circumstance, along with a significant decrease in the scattered light intensity from microfiltered water (see Fig. 3), confirms our suggestion about the relationship of the hexamer water structure (characteristic of ice) with the presence of bubstons and bubston clusters in water. Therefore, microcapillary water filtering and the corresponding decrease in the concentration of hexagonal structural elements in water should distort the Raman scattering profile. In this case, one would expect a decrease in the intensity of the low-frequency wing ($\nu \approx 3200$ cm^{-1}) of the spontaneous Raman scattering line and, correspondingly, an increase in the intensity of its high-frequency wing ($\nu \approx 3400-3500$ cm^{-1}). This distortion of the Raman spectrum in water should lead to an increase in the SRS gain at the frequencies corresponding to the vibrations of small complexes, and, therefore, a decrease in the SRS threshold at these frequencies.

To verify this statement, we determined the SRS threshold energies in water samples of different compositions (Fig. 7). As one would expect, the energy at which SRS occurs in the water subjected to microcapillary filtering turned out to be almost half of that for the water contacting with atmosphere. This result indicates that the transformation of the molecular water structure allows one to obtain water with a low SRS threshold.

Along with the results obtained by studying the capillary water, an issue of particular interest is the investigation of the optical breakdown in the field of USLPs at the fundamental frequency of the YAG:Nd^{3+} laser (λ = 1064 nm) in this water. To this end, a single 20-ps pulse at the fundamental wavelength (λ = 1064 nm) of the YAG:Nd^{3+} laser was introduced into water-filled cell C (see Fig. 1) through focusing lens L1, with filter F1 removed. Signal S of the radiation scattered in the cell was recorded at an angle of 90° with respect to the incident beam using photodetector PD. Figure 8 shows the dependence of the scattering signal intensity on the energy of incident picosecond pulse for that water that was in contact with atmosphere for a long time and for the water subjected

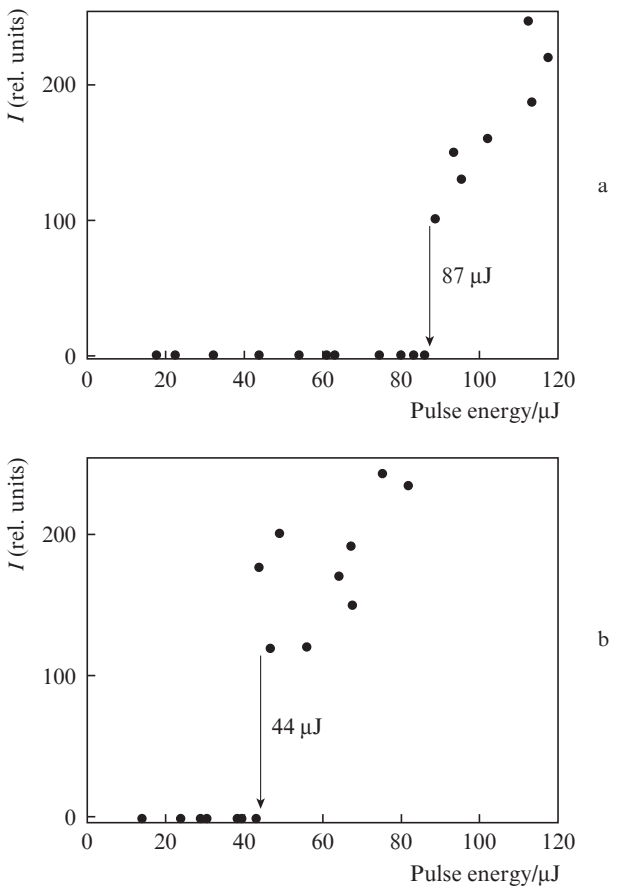

Figure 7. Dependences of the intensity of the SRS signal, arising only in the forward SRS regime in (a) water contacting with atmosphere and (b) water subjected to track membrane microfiltration, on the energy of excitation picosecond laser pulse. The SRS threshold energies are indicated by arrows.

to microcapillary filtration. The existence of the optical breakdown in water is evidenced by a sharp increase in the scattering signal intensity from the focal region of laser beam waist. It can be seen in Fig. 8 that the threshold breakdown energy E_{th} for the capillary water is 0.5 mJ, a value greatly exceeding that for the water contacting with atmosphere (E_{th} = 0.05 mJ). Hence, the capillary water has a higher optical strength. This feature, along with a lower SRS threshold, makes this water a promising tool for studying the nonlinear optics of liquids in strong light fields.

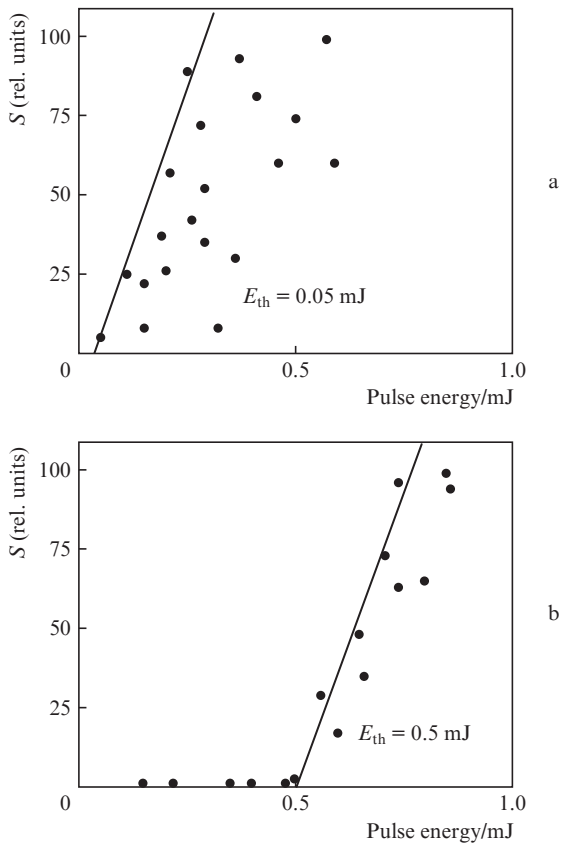

Figure 8. Dependences of the scattering signal on the energy of the excitation picosecond pulse at a wavelength λ = 1064 nm for (a) water contacting with atmosphere for a long time and (b) water subjected to microcapillary filtration.

Thus, the results of this study showed that the use of SRS in the field of a single picosecond pulse can be used for microscopic description of the water structure. The SRS analysis revealed structural features of water contacting with atmosphere and water subjected to microcapillary filtration. Our experiments showed a relationship of the hexagonal structure that is characteristic of ice and observed in water with the presence of bubstons and bubston clusters in water.

References

1. Huang C., Wikfeldt K.T., TokushimaT., Nordlund D., Harada Y., et al. *Proc. Natl. Sci. USA*, **106** (36), 15214 (2009).
2. Nilsson A., Pettersson L.G.M. *Chem. Phys.*, **389**, 1 (2011).
3. Pershin S.M., Bunkin A.F., Luk'yanchenko V.A. *Quantum Electron.*, **40**, 1146 (2010) [*Kvantovaya Elektron.*, **40**, 1146 (2010)].
4. Wei Xing, Miranda Paulo B., Shen Y.R. *Phys. Rev. Lett.*, **86**, 1554 (2001).
5. Goh M.C., Hicks J.M., Kemnitz K., Pinto G.R., Bhattacharyya K., Eisenthal K.B., Heinz T.F. *J. Phys. Chem.*, **92**, 5074 (1988).
6. Walrafen G.E. *J. Chem. Phys.*, **47**, 114 (1967).
7. Colles M.J., Walrafen G.E., Wecht K.W. *Chem. Phys. Lett.*, **4**, 621 (1970).
8. Rahn O., Maier M., Kaiser W. *Opt. Commun.*, **1**, 109 (1969).
9. Bespalov V.I., Kerevkin Yu.K., Pasmanik G.A. *Opt. Spectrosc.*, **38**, 643 (1975).
10. Sceats M., Rice S.A., Butler J.E. *J. Chem. Phys.*, **63**, 5390 (1975).
11. Montrose C.J., Bucaro J.A., Marschall-Coakley J., Litovitz T.A. *J. Chem. Phys.*, **60**, 5025 (1974).
12. Hindman J.C., Zielen A.J., Svirmickas A., Wood M. *J. Chem. Phys.*, **54**, 621 (1971).
13. Bunkin N.F., Bunkin F.V. *Zh. Eksp. Teor. Fiz.*, **74**, 271 (1992).
14. Babenko V.A., Bunkin N.F., Suyazov N.V., Sychev A.A. *Quantum Electron.*, **37** (9), 804 (2007) [*Kvantovaya Elektron.*, **37** (9), 804 (2007)].
15. Yurchenko S.O., Shkirin A.V., Ninham B.W., Sychev A.A., Babenko V.A., Penkov N.V., Kryuchkov N.P., Bunkin N.F. *Langmuir*, **32**, 11245 (2016).
16. Bunkin N.F., Shkirin A.V., Suyazov N.V., Babenko V.A., Sychev A.A., Penkov N.V., Belosludtsev K.N., Gudkov S.V. *J. Phys. Chem. B*, **120**, 1291 (2016).
17. Kelsall G.H., Tang S., Yurdakul S., Smith A. *J. Chem. Soc., Faraday Trans.*, **92**, 3887 (1996).
18. Babenko V.A., Sychev A.A. *J. Rus. Laser Res.*, **20**, 478 (1999).